

Classical problems in the theory of elasticity and the quantum theory of angular momentum

S V Goupalov

DOI: <https://doi.org/10.3367/UFNe.2019.04.038562>

Contents

1. Introduction	57
2. Notion of angular momentum for a classical vector field	57
3. Spherical waves in a homogeneous isotropic medium	59
4. Free vibrations of a sphere	60
5. Cylindrical waves in a homogeneous isotropic elastic medium	61
6. Vibrations of an infinite rod with a free surface	62
7. Vibrations of an infinite plate with free surfaces	63
8. Conclusions	65
References	65

Abstract. We show that applying the methods of the quantum theory of angular momentum enables us to obtain frequency equations for vibrational modes of a uniform isotropic elastic sphere, cylindrical rod, and infinite plate and results in a natural classification of these modes. We discuss how these models can be applied to describe vibrations of metal nanoparticles and semiconductor nanocrystals.

Keywords: quantum theory of angular momentum, theory of elasticity, vibrational modes, metal nanoparticles, semiconductor nanocrystals, nanorods, nanoplatelets

*In memory of Igor' Aleksandrovich Merkulov
(1947–2014)*

1. Introduction

We discuss free vibrational modes of homogeneous isotropic elastic bodies: a sphere, an infinite cylindrical rod, and an infinite plate. The rod and the plate are not assumed to be thin, in contrast, e.g., to [1]. Problems on finding free vibration frequencies in such elastic bodies were mostly solved in the last quarter of the 19th century. The original papers devoted to their solution by outstanding scientists of that time [2–8] are written in an archaic mathematical language if viewed from the present-day perspective. Granted, there are accessible surveys of their results, aimed first and foremost at engineers [9, 10] and seismologists [11]. However, as we show in what follows, these results can be obtained most naturally

with the help of the mathematical formalism of the quantum theory of angular momentum [12]. This mathematical formalism, developed in the first half of the 20th century, is a *lingua franca* for physicists working in very different areas.

Recent progress in nanotechnology has led to wide dissemination of quasi-zero-dimensional, quasi-one-dimensional, and quasi-two-dimensional structures, produced, for example, by the methods of colloidal chemistry and used in a broad spectrum of applications in optoelectronics and medicine. Low-frequency vibrational modes in these nanostructures can be approximately described using the models of a homogeneous elastic sphere, rod, or plate. Quanta of low-frequency vibrations in nanostructures, or phonons, take part in many physical processes that respect conservation laws for angular momentum and/or its projection. Importantly, the conservation laws deal with the total phonon angular momentum. We demonstrate that the indices used to classify vibrational modes in classical problems of elasticity theory correspond to quantum numbers of the total angular momentum or its projection for quanta of respective vibrations.

On the other hand, problems on free vibrational modes in ideal elastic bodies are of independent interest. For example, even though in modern seismology Earth is described with essentially more complicated models that take gravity and rotation into account, the classification of modes proposed in the original work of Lamb [3] is still used to describe vibrations excited in earthquakes¹ [11].

2. Notion of angular momentum for a classical vector field

The notions of orbital momentum and spin, as applied to classical vector fields, are frequently introduced by considering electromagnetic fields [13–15]. We begin with a scalar field

S V Goupalov Ioffe Institute,
ul. Politekhnicheskaya 26, 194021 Saint Petersburg, Russian Federation;
Department of Physics, Jackson State University,
Jackson MS 39217, USA
E-mail: goupalov@coherent.ioffe.ru

Received 24 February 2019, revised 8 April 2019
Uspekhi Fizicheskikh Nauk 190 (1) 63–72 (2020)
Translated by S D Danilov; edited by A M Semikhatov

¹ The site <https://saviot.cnrs.fr/terre/index.en.html>, maintained by Saviot, proposes a computer animation of Earth vibrational modes based on the model of a homogeneous elastic sphere.

$f(\mathbf{r})$ and analyze its behavior under the rotation of coordinate axes of a Cartesian system through a small angle $\delta\theta$ about the direction defined by a unit vector \mathbf{n} . This rotation transforms the coordinate unit vectors in the first order in $\delta\theta$ as

$$\mathbf{e}'_\alpha = \mathbf{e}_\alpha + \delta\theta \mathbf{n} \times \mathbf{e}_\alpha, \quad (1)$$

where $\alpha = x, y, z$. In the new coordinate system, the point \mathbf{r} has the Cartesian coordinates (x', y', z') :

$$\mathbf{r} = x\mathbf{e}_x + y\mathbf{e}_y + z\mathbf{e}_z = x'\mathbf{e}'_x + y'\mathbf{e}'_y + z'\mathbf{e}'_z. \quad (2)$$

If we now consider the coordinates and unit vectors as functions of the coordinate system rotation angle θ , we obtain

$$\mathbf{r} = x(\theta)\mathbf{e}_x(\theta) + y(\theta)\mathbf{e}_y(\theta) + z(\theta)\mathbf{e}_z(\theta) = \text{const}. \quad (3)$$

Equation (1) implies that

$$\frac{d\mathbf{e}_\alpha}{d\theta} = \mathbf{n} \times \mathbf{e}_\alpha. \quad (4)$$

Using it and differentiating (3) yields

$$\frac{d\mathbf{r}}{d\theta} = \frac{\partial\mathbf{r}}{\partial\theta} + \mathbf{n} \times \mathbf{r} = 0. \quad (5)$$

The rotation of the coordinate system does not affect the value of a scalar field at a point \mathbf{r} , but the coordinates change and hence the functional dependence of the scalar field on the coordinates also changes. We can therefore write

$$f_\theta(x(\theta), y(\theta), z(\theta)) = \text{const}, \quad (6)$$

where the subscript in f_θ emphasizes this dependence. Differentiating equality (6) with respect to θ , we find

$$\frac{df}{d\theta} = \frac{\partial f}{\partial\theta} + \frac{\partial\mathbf{r}}{\partial\theta} \nabla f = \frac{\partial f}{\partial\theta} - (\mathbf{n} \times \mathbf{r}) \nabla f = \frac{\partial f}{\partial\theta} - \mathbf{n}(\mathbf{r} \times \nabla f) = 0, \quad (7)$$

where we used (5). The last equality in (7) can be rewritten as

$$-i \frac{\partial f}{\partial\theta} = \mathbf{n} \hat{\mathbf{L}} f, \quad (8)$$

where the differential operator

$$\hat{\mathbf{L}} = -i \mathbf{r} \times \nabla \quad (9)$$

coincides with the quantum orbital angular momentum operator up to a factor of \hbar . In particular, it follows from (8) that

$$\hat{L}_z f = -i \frac{\partial f}{\partial\varphi}, \quad (10)$$

where φ is the azimuthal angle of a spherical or cylindrical coordinate system.

As is well known [12, 13], the common eigenfunctions of the operators $\hat{\mathbf{L}}^2$ and \hat{L}_z are the spherical harmonics

$$\hat{\mathbf{L}}^2 Y_{l_z} \left(\frac{\mathbf{r}}{r} \right) = l(l+1) Y_{l_z} \left(\frac{\mathbf{r}}{r} \right), \quad \hat{L}_z Y_{l_z} \left(\frac{\mathbf{r}}{r} \right) = l_z Y_{l_z} \left(\frac{\mathbf{r}}{r} \right). \quad (11)$$

We now turn to the transformation of a vector field $\mathbf{A}(\mathbf{r})$. By analogy with (6), we can write

$$\frac{d}{d\theta} \left[\sum_{\alpha=x,y,z} A_{\theta\alpha}(x(\theta), y(\theta), z(\theta)) \mathbf{e}_\alpha(\theta) \right] = 0, \quad (12)$$

or

$$\frac{\partial\mathbf{A}(\mathbf{r})}{\partial\theta} + \left(\frac{\partial\mathbf{r}}{\partial\theta} \nabla \right) \mathbf{A} + \mathbf{n} \times \mathbf{A} = 0, \quad (13)$$

whence it follows that

$$-i \frac{\partial\mathbf{A}}{\partial\theta} = (\mathbf{n} \hat{\mathbf{L}}) \mathbf{A} + i \mathbf{n} \times \mathbf{A} \equiv (\mathbf{n} \hat{\mathbf{L}}) \mathbf{A} + (\mathbf{n} \hat{\mathbf{S}}) \mathbf{A}. \quad (14)$$

The last term in the right-hand side of (14) occurs because the Cartesian components of a vector field mix under a rotation of coordinate axes. It can be readily seen that $\hat{\mathbf{S}}$, up to \hbar , coincides with the quantum spin operator for a particle with the spin $s = 1$. In particular, if $\mathbf{A}(\mathbf{r})$ is written as a column vector, we obtain

$$i \mathbf{n} \times \mathbf{A} = (\mathbf{n} \hat{\mathbf{S}}) \mathbf{A} = i \begin{pmatrix} 0 & -n_z & n_y \\ n_z & 0 & -n_x \\ -n_y & n_x & 0 \end{pmatrix} \begin{pmatrix} A_x \\ A_y \\ A_z \end{pmatrix}. \quad (15)$$

The matrices corresponding to the components $\hat{S}_x, \hat{S}_y, \hat{S}_z$ coincide with the matrices of Cartesian spin operator components for a particle with $s = 1$ in a Cartesian basis [12]. The equalities

$$\hat{\mathbf{S}}^2 = \hat{S}_x^2 + \hat{S}_y^2 + \hat{S}_z^2 = 2\hat{I} = s(s+1)\hat{I} \quad (16)$$

hold, where \hat{I} is the unit matrix. The operator \hat{S}_z has the eigenvalues $\pm 1, 0$; their eigenvectors can be conveniently chosen as cyclic unit vectors [12]:

$$\mathbf{e}_{+1} = -\frac{\mathbf{e}_x + i\mathbf{e}_y}{\sqrt{2}}, \quad \mathbf{e}_0 = \mathbf{e}_z, \quad \mathbf{e}_{-1} = \frac{\mathbf{e}_x - i\mathbf{e}_y}{\sqrt{2}}. \quad (17)$$

Expression (14) can be rewritten as

$$-i \frac{\partial\mathbf{A}}{\partial\theta} = (\mathbf{n} \hat{\mathbf{J}}) \mathbf{A}, \quad (18)$$

where $\hat{\mathbf{J}} = \hat{\mathbf{L}} + \hat{\mathbf{S}}$ is an analog of the operator of the total angular momentum.

We emphasize that $\hat{\mathbf{L}}, \hat{\mathbf{S}},$ and $\hat{\mathbf{J}}$ are dimensionless operators related to the operator of infinitesimal rotation acting on a classical vector field. They are identified with the angular momentum only in quantum mechanics through their redefinition by multiplication by \hbar , whereby they acquire the required dimension. However, having the established quantum mechanical terminology in mind, it is difficult to resist calling these operators angular momentum operators if they are also applied to classical vector fields. We take these liberties in what follows.

Depending on the symmetry of the elasticity theory problems to be solved, the conservation law for either the total angular momentum or its projection on the z axis holds. The vector displacement field for free vibrational modes is an eigenvector of the operator $\hat{\mathbf{J}}^2$ and/or the operator \hat{J}_z , and the respective eigenvalues are analogs of quantum numbers that can be used to classify the modes. Because all commutation relations among the components of the angular momentum operator are the same as in quantum mechanics (up to \hbar), the notion of a ‘good quantum number’ is generally very productive in the problems of our interest. Finally, as is known [13], the properties of eigenvalues of the angular momentum operator are fully defined by the commutation relations for these operators. Thus, the eigenvalues of $\hat{\mathbf{J}}^2$ can be written as $j(j+1)$, where j is a nonnegative integer number (in general, half-integer values are possible for j ; however,

they are ruled out for the spin $s = 1$), and eigenvalues of \hat{J}_z are the integer numbers in the range from $-j$ to j .

The eigenvectors (strictly speaking, they are vector fields, but we call them vectors for brevity) of the operators $\hat{\mathbf{J}}^2$ and \hat{J}_z (and also of the operators $\hat{\mathbf{L}}^2$ and \hat{S}^2) can be constructed from the eigenfunctions of $\hat{\mathbf{L}}^2$ and \hat{L}_z and eigenvectors of $\hat{\mathbf{S}}^2$ and \hat{S}_z with the help of the Wigner $3jm$ symbols [12]:

$$\mathbf{Y}_{jm}^l\left(\frac{\mathbf{r}}{r}\right) = (-1)^{s-l+m} \sqrt{2j+1} \sum_{\sigma, l_z} \begin{pmatrix} s & l & j \\ \sigma & l_z & -m \end{pmatrix} Y_{l_z}^s\left(\frac{\mathbf{r}}{r}\right) \mathbf{e}_\sigma. \quad (19)$$

These eigenvectors are known as vector spherical harmonics or spherical vectors [12]. Just like ordinary spherical harmonics, they depend only on the angles of the vector \mathbf{r} .

In the same way as the operators $\hat{\mathbf{L}}$, $\hat{\mathbf{S}}$, and $\hat{\mathbf{J}}$ are related to the behavior of scalar and vector fields under coordinate system rotation, the notion of parity is related to their behavior under coordinate system inversions [16]. The action of the inversion operator on a scalar field $f(\mathbf{r})$ amounts only to the change of sign of the coordinates, $\hat{P}f(\mathbf{r}) = f(-\mathbf{r})$. For the action on a vector field $\mathbf{A}(\mathbf{r})$, it has to be additionally taken into account that the reversal of the axes also changes the sign of all vector components. Hence, $\hat{P}\mathbf{A}(\mathbf{r}) = -\mathbf{A}(-\mathbf{r})$ [16]. Accordingly, the parity of vector spherical harmonics is such that [12]

$$\hat{P}\mathbf{Y}_{jm}^l\left(\frac{\mathbf{r}}{r}\right) = (-1)^{l+1} \mathbf{Y}_{jm}^l\left(\frac{\mathbf{r}}{r}\right). \quad (20)$$

Ignoring this trivial property of vector spherical harmonics can lead to ambiguities [17].

The eigenfunctions of $\hat{\mathbf{L}}^2$ and \hat{L}_z can be refined such that they contain a radial part and in addition satisfy the Helmholtz equation and are finite at $r = 0$. This is achieved by multiplying spherical harmonics $Y_{l_z}^s$ by

$$\sqrt{\frac{2}{\pi}} j_l(kr),$$

where $j_l(x)$ is the spherical Bessel function, k is the wave number, and $\sqrt{2/\pi}$ is the normalization factor. Then the eigenvectors of the operators $\hat{\mathbf{J}}^2$, \hat{J}_z , $\hat{\mathbf{L}}^2$, and $\hat{\mathbf{S}}^2$ that we construct take the form

$$\mathbf{u}_{jmk}^l(\mathbf{r}) = \sqrt{\frac{2}{\pi}} j_l(kr) \mathbf{Y}_{jm}^l\left(\frac{\mathbf{r}}{r}\right). \quad (21)$$

3. Spherical waves in a homogeneous isotropic medium

The equations of motion of an isotropic elastic medium [1] can be conveniently written in the operator form [18]

$$\hat{A}\mathbf{u} \equiv \left[(c_1^2 - c_t^2)(\hat{\mathbf{S}}\nabla)^2 - c_1^2 \hat{\Delta} \right] \mathbf{u} = \omega^2 \mathbf{u}, \quad (22)$$

where $\mathbf{u}(\mathbf{r}, t)$ is the vector displacement field, which is supposed to vary harmonically with time at a frequency ω , c_1 and c_t are the longitudinal and transverse speeds of sound [1], and Δ is the scalar Laplacian. Just as in Eqn (15), $\mathbf{u}(\mathbf{r}, t)$ is here understood as a column vector, but we should keep in mind that Eqn (22) holds for any coordinate system, not only Cartesian ones. Because we are only interested in monochromatic solutions of the equations of motion, the time dependence of $\mathbf{u}(\mathbf{r}, t)$ is suppressed.

Equations (22) have spherical symmetry. As a consequence, they describe motion with conserved total angular

momentum. This can be seen formally from the fact that the operators \hat{A} and $\hat{\mathbf{J}}^2$ commute. In this sense, j is a good quantum number. The other good quantum numbers are the projection of the total angular momentum m on a selected direction, which is the z axis in our case, and the parity. Together with the frequency squared ω^2 , they form a full set of eigenvalues of mutually commuting operators. However, the orbital momentum is not conserved in the motion described by Eqn (22). According to the momentum summation rule in quantum mechanics, the total momentum j and spin $s = 1$ allow the values of the orbital momentum $l = j, j \pm 1$, and the values j and $j \pm 1$ are related to solutions with different parities. For this reason, in the basis of functions (21), the operator \hat{A} splits into 3×3 blocks that correspond to a nonzero j and some definite value of m and have the following form:

$$\begin{array}{c|ccc} & l & j-1 & j+1 & j \\ \hline j-1 & * & * & * & 0 \\ \hline j+1 & * & * & * & 0 \\ \hline j & 0 & 0 & 0 & * \end{array}, \quad (23)$$

where asterisks (*) denote nonzero matrix entries. The case $j = 0$ is special; the operator \hat{A} in basis (21) then takes the form

$$\begin{array}{c|c} & l & 1 \\ \hline 1 & * & * \end{array}. \quad (24)$$

We thus can conclude that in two cases ($l = j$ and $j = 0, l = 1$) $\mathbf{u}_{jmk}^l(\mathbf{r})$ is an eigenvector of the operator \hat{A} . We now find its eigenvalues in these cases. As is known [1], in an unbounded isotropic elastic medium there are two types of propagating waves: longitudinal and transverse. Accordingly, the eigenvalues of \hat{A} can be given by $c_1^2 k^2$ and $c_t^2 k^2$. For a plane wave, the notions of ‘longitudinal’ and ‘transverse’ are defined with respect to the direction of the wave vector. For an arbitrary vector field $\mathbf{A}(\mathbf{r})$, this notion can be generalized by assuming that longitudinal and transverse vector fields satisfy the respective conditions $\nabla \times \mathbf{A} = 0$ and $\nabla \mathbf{A} = 0$. It can be easily verified that the field

$$\mathbf{u}_{jmk}^{(2)}(\mathbf{r}) \equiv \mathbf{u}_{jmk}^j(\mathbf{r}) \quad (25)$$

is transverse, and the field $\mathbf{u}_{00k}^{(1)}(\mathbf{r}) \equiv \mathbf{u}_{00k}^1(\mathbf{r})$ is longitudinal.

It remains to diagonalize the 2×2 block in (23). For a plane elastic wave propagating in a given direction, three orthogonal linear polarizations are possible: one longitudinal and two transverse. Obviously, the same degeneration takes place for a spherical wave with fixed values of the total angular momentum j and its projection m . We have already found that solution (25) of Eqn (22) is transverse. Hence, one of the remaining solutions is transverse and the other longitudinal. To find them, it suffices to write linear combinations of $\mathbf{u}_{jmk}^{j+1}(\mathbf{r})$ and $\mathbf{u}_{jmk}^{j-1}(\mathbf{r})$ and require that either their divergence or curl vanish. As a result, for the longitudinal solution we have [18]

$$\mathbf{u}_{jmk}^{(1)}(\mathbf{r}) = \sqrt{\frac{j+1}{2j+1}} \mathbf{u}_{jmk}^{j+1}(\mathbf{r}) + \sqrt{\frac{j}{2j+1}} \mathbf{u}_{jmk}^{j-1}(\mathbf{r}), \quad (26)$$

and for the transverse one,

$$\mathbf{u}_{jmk}^{(11)}(\mathbf{r}) = \sqrt{\frac{j}{2j+1}} \mathbf{u}_{jmk}^{j+1}(\mathbf{r}) - \sqrt{\frac{j+1}{2j+1}} \mathbf{u}_{jmk}^{j-1}(\mathbf{r}). \quad (27)$$

In addition to solutions (25)–(27), which are longitudinal and transverse with respect to the operator \mathbf{V} , we can construct eigenvectors of $\hat{\mathbf{J}}^2$ and \hat{J}_z that are longitudinal or transverse with respect to the vector \mathbf{r} [12]. The linearly independent transverse vectors have the form [12]

$$\mathbf{Y}_{jm}^{(1)}\left(\frac{\mathbf{r}}{r}\right) = \sqrt{\frac{j+1}{2j+1}} \mathbf{Y}_{jm}^{j-1}\left(\frac{\mathbf{r}}{r}\right) + \sqrt{\frac{j}{2j+1}} \mathbf{Y}_{jm}^{j+1}\left(\frac{\mathbf{r}}{r}\right), \quad (28)$$

$$\mathbf{Y}_{jm}^{(0)}\left(\frac{\mathbf{r}}{r}\right) = \mathbf{Y}_{jm}^j\left(\frac{\mathbf{r}}{r}\right), \quad (29)$$

and the longitudinal vector is

$$\mathbf{Y}_{jm}^{(-1)}\left(\frac{\mathbf{r}}{r}\right) = \sqrt{\frac{j}{2j+1}} \mathbf{Y}_{jm}^{j-1}\left(\frac{\mathbf{r}}{r}\right) - \sqrt{\frac{j+1}{2j+1}} \mathbf{Y}_{jm}^{j+1}\left(\frac{\mathbf{r}}{r}\right). \quad (30)$$

It can be readily seen that these spherical vectors also have a certain parity. On the sphere, vector (30) is directed along the normal to the surface, and vectors (28) and (29) lie in the tangent plane.

4. Free vibrations of a sphere

To find the eigenfrequencies of free oscillations of a sphere with radius R , we take a linear combination of independent solutions of Eqn (22) that correspond to a given frequency ω , the total angular momentum j , its projection m , and parity, and require that the corresponding traction vector vanish on the sphere, i.e., at $r = R$. In our case, the independent solutions of (22) corresponding to the parity $(-1)^j$ are given by expressions (26) and (27), and the solution with the parity $(-1)^{j+1}$ is given by (25). The longitudinal solution should be taken with the wave number $k = \omega/c_l \equiv q$ and the transverse ones with $k = \omega/c_t \equiv Q$, as shown schematically in Fig. 1.

The modes coming from solution (25) are purely transverse. They are known as torsional or toroidal vibrations. These modes are frequently denoted as ${}_n T_j^m$ [11], where n is the ‘principal quantum number’ taking the value $n = 0$ for the fundamental mode and $n > 0$ for overtones.²

The modes coming from solutions (26) and (27) are mixed. They are called spheroidal vibrations and are denoted as ${}_n S_j^m$ [11]. The spheroidal modes ${}_n S_0^0$ are an exception: they are longitudinal. These modes describe radial vibrations, and the fundamental mode ${}_0 S_0^0$ is also called a ‘breathing’ one.³

Having clarified the structure of solutions, we can put parity considerations aside in order to obtain the characteristic equation for the frequencies of all vibrational modes simultaneously. The force per unit area of the sphere due to stresses

$$\mathbf{F}_{jm} = \sigma_{rr} \mathbf{e}_r + \sigma_{r\theta} \mathbf{e}_\theta + \sigma_{r\varphi} \mathbf{e}_\varphi \quad (31)$$

² Sometimes the modes are numbered starting from $n = 1$ instead of $n = 0$.

³ The site <https://saviot.cnrs.fr/lamb/index.en.html>, maintained by Saviot, offers online computations of frequencies of all possible vibrational modes for spheres made of various materials and visualizes the patterns of the displacement field associated with these vibrations.

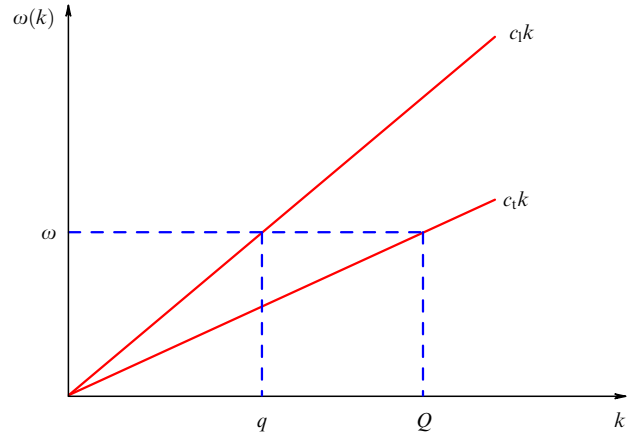


Figure 1. Longitudinal and transverse elastic waves can propagate in a homogeneous and isotropic elastic medium; therefore, there are two wave numbers for each frequency of harmonic oscillation.

(where σ_{rr} , $\sigma_{r\theta}$, and $\sigma_{r\varphi}$ are the components of stress tensor [1] in a spherical coordinate system, and \mathbf{e}_r , \mathbf{e}_θ , and \mathbf{e}_φ are the corresponding unit coordinate vectors), which corresponds to the linear combination

$$a \mathbf{u}_{jmq}^{(1)}(\mathbf{r}) + b \mathbf{u}_{jmQ}^{(11)}(\mathbf{r}) + c \mathbf{u}_{jmQ}^{(12)}(\mathbf{r})$$

of solutions (26), (27), and (25), can be conveniently written as a decomposition in vector spherical harmonics (28)–(30),

$$\begin{aligned} \mathbf{F}_{jm} = & -\rho_M \sqrt{\frac{2}{\pi}} \mathbf{Y}_{jm}^{(-1)}\left(\frac{\mathbf{r}}{r}\right) \left\{ a \left[(c_l^2 - 2c_t^2) q j_j(qR) \right. \right. \\ & \left. \left. - \frac{2c_t^2}{q} \frac{d^2 j_j(qR)}{dR^2} \right] + b 2c_t^2 \sqrt{j(j+1)} \frac{d}{dR} \left(\frac{j_j(QR)}{QR} \right) \right\} \\ & + \rho_M \sqrt{\frac{2}{\pi}} c_t^2 \mathbf{Y}_{jm}^{(1)}\left(\frac{\mathbf{r}}{r}\right) \left\{ a 2 \sqrt{j(j+1)} \frac{d}{dR} \left(\frac{j_j(qR)}{qR} \right) \right. \\ & \left. - b \left[\frac{1}{Q} \frac{d^2 j_j(QR)}{dR^2} + (j^2 + j - 2) \frac{j_j(QR)}{QR^2} \right] \right\} \\ & + c \rho_M \sqrt{\frac{2}{\pi}} c_t^2 \mathbf{Y}_{jm}^{(0)}\left(\frac{\mathbf{r}}{r}\right) QR \frac{d}{dR} \left(\frac{j_j(QR)}{QR} \right), \quad (32) \end{aligned}$$

where ρ_M is the density of the sphere material. From expression (32), we can immediately conclude that solutions with different parities are not mixed via the boundary conditions on the sphere surface, where force (32) vanishes.

At $j = 0$, the condition $\mathbf{F}_{00} = 0$ yields the equation for the frequencies of radial vibrations of the sphere [1]:

$$\frac{\tan(qR)}{qR} = \frac{1}{1 - [c_l q R / (2c_t)]^2}. \quad (33)$$

This result was already known to Poisson [19]. A full analysis of free oscillations of a sphere was given in Refs [2–4].

For the frequencies of torsional or toroidal vibrations, the condition $\mathbf{F}_{jm} = 0$ gives

$$\frac{d}{dR} \left(\frac{j_j(QR)}{QR} \right) = 0 \quad (34)$$

or [10, 11]

$$(j-1) j_j(QR) - QR j_{j+1}(QR) = 0. \quad (35)$$

Finally, for spheroidal vibrations with $j > 0$, it follows from the condition $\mathbf{F}_{jm} = 0$ that [10, 11]

$$\begin{aligned} & j_j(qR)j_j(QR)(QR)^2 \left[(j-1)(2j+1) - \frac{(QR)^2}{2} \right] \\ & + 2j_{j+1}(qR)j_{j+1}(QR)(qR)(QR)(j-1)(j+2) \\ & + j_j(qR)j_{j+1}(QR)QR \left[(QR)^2 - 2j(j-1)(j+2) \right] \\ & + 2j_{j+1}(qR)j_j(QR)qR \left[(QR)^2 - (j^2-1)(j+2) \right] = 0. \quad (36) \end{aligned}$$

As j increases, spherical harmonics entering expressions (26) and (27) oscillate more and more strongly, such that, starting with some value of j , the waves described by them become so short that the sphere curvature is no longer important for them. It can be shown [10, 11] that as $j \rightarrow \infty$, Eqn (36) transforms into the characteristic equation for Rayleigh waves propagating along a plane interface of an elastic medium filling a half-space.

The analysis we carried out can be applied to describe free vibrations of spherical nanoparticles. Nanocrystals of semiconductors of a spherical form were first synthesized by Ekimov and Onushchenko in glass matrices as a result of a thermally induced diffusive phase transition of an over-saturated solid solution [20]. Afterwards, methods relying on synthesis of semiconductor and metal nanocrystals from colloidal solutions were proposed [21].

Vibrational modes in such nanocrystals can be excited in experiments on low-frequency Raman scattering. According to the selection rules [17, 18, 22], spheroidal modes with $j = 0$ and $j = 2$ are excited in such experiments. Because the longitudinal speed of sound always exceeds the transverse one ($c_l > c_t$) [1], the frequency of the fundamental mixed mode ${}_0S_2^m$ is lower than the frequency of the fundamental ‘breathing’ mode ${}_0S_0^0$, which is purely longitudinal. Review [23] is dedicated to the study of vibrations in spherical semiconductor nanocrystals and metallic nanoparticles with the help of low-frequency Raman scattering.

Another way of exciting vibrations in metallic nanoparticles is used in pump-probe experiments that study linear light absorption after the action of a powerful femtosecond laser pumping pulse. Under these conditions, the excitation of the electron subsystem in metallic nanoparticles by a short pumping pulse is accompanied by energy transfer from the electron subsystem to the crystal lattice for several picoseconds. This time interval is shorter than the period of free vibrations of spherical nanoparticles. Therefore, heating and fast expansion of the crystal lattice excite the vibrational modes. In turn, vibrations of nanoparticles lead to the dependence of absorption of the probing pulse on the time lag relative to the pumping pulse. This dependence comes from changes in the volumes of nanoparticles that accompany their spheroidal vibrations, causing periodic modulation in the frequency of the nanoparticle surface plasmon resonance. This allows measuring the nanoparticle free vibration frequency. Radial vibrations, which have a purely longitudinal character, i.e., are accompanied by expansions and compressions, are excited and detected most efficiently. Such experiments are described in review [24].

Nanoparticles are so small that they frequently turn out to be monocrystals. Crystal anisotropy begins playing a role then, because the symmetry of the crystal lattice is lower than spherical symmetry. Strictly speaking, the isotropic model becomes inapplicable in this case. However, by changing the

degree of anisotropy in numerical modeling, we can learn how the modes of vibrations evolve under the transition from an isotropic system to an anisotropic one [23]. In this case, splitting and shifts in frequencies of individual modes of vibrations are observed. Some materials have a relatively weak crystal anisotropy, which justifies the use of the isotropic model for their vibration analysis. Furthermore, nanoparticles of some materials, for example, silver, commonly consist of several randomly oriented crystallites or grains [23]. In this case, their vibrations are well described by the isotropic model that involves the speeds of sound averaged along various crystal directions as parameters. Finally, for experiments with ensembles of nanoparticles characterized by a broad distribution over sizes, the crystal anisotropy effect might be too fine to take it into account.

5. Cylindrical waves in a homogeneous isotropic elastic medium

We find linearly independent solutions of Eqn (22) that correspond to some definite values of the frequency ω , the projection m of the total angular momentum on the z axis, and the projection k_z of the wave vector on the z axis. We start with the equality $\hat{J}_z = \hat{L}_z + \hat{S}_z$. The eigenvectors of \hat{S}_z are given in (17), and eigenfunctions (not normalized) of \hat{L}_z , according to definition (10), are written as $\exp(i l_z \varphi)$. As a consequence, it is convenient to characterize a point in space with the help of a cylindrical coordinate system $\mathbf{r} = (\rho, \varphi, z)$ and represent the displacement vectors as column vectors in cyclic basis (17). We require the solutions to be finite on the z axis (i.e., for $\rho = 0$) and refine the eigenfunctions of \hat{L}_z such that they satisfy the two-dimensional Helmholtz equation with the wave number k_\perp . This is achieved by multiplying the functions $\exp(i l_z \varphi)$ by the Bessel functions $J_l(k_\perp \rho)$. We take into account that one of the solutions has to be longitudinal with respect to the operator ∇ , and the two others should be transverse. It can be readily seen that these conditions are satisfied by the following solutions [25]:

$$\begin{aligned} \mathbf{u}_{mk_\perp k_z}^{(l)}(\rho, \varphi, z) &= \frac{\exp[i(k_z z + m\varphi)]}{\sqrt{2\pi}\sqrt{k_\perp^2 + k_z^2}} \\ &\times \begin{pmatrix} \frac{k_\perp}{\sqrt{2}} \exp(-i\varphi) J_{m-1}(k_\perp \rho) \\ -i k_z J_m(k_\perp \rho) \\ \frac{k_\perp}{\sqrt{2}} \exp(i\varphi) J_{m+1}(k_\perp \rho) \end{pmatrix}, \quad (37) \end{aligned}$$

$$\begin{aligned} \mathbf{u}_{mk_\perp k_z}^{(t1)}(\rho, \varphi, z) &= \frac{\exp[i(k_z z + m\varphi)]}{\sqrt{2\pi}\sqrt{k_\perp^2 + k_z^2}} \\ &\times \begin{pmatrix} \frac{k_z}{\sqrt{2}} \exp(-i\varphi) J_{m-1}(k_\perp \rho) \\ i k_\perp J_m(k_\perp \rho) \\ \frac{k_z}{\sqrt{2}} \exp(i\varphi) J_{m+1}(k_\perp \rho) \end{pmatrix}, \quad (38) \end{aligned}$$

$$\begin{aligned} \mathbf{u}_{mk_\perp k_z}^{(t2)}(\rho, \varphi, z) &= \frac{\exp[i(k_z z + m\varphi)]}{2\sqrt{\pi}} \\ &\times \begin{pmatrix} \exp(-i\varphi) J_{m-1}(k_\perp \rho) \\ 0 \\ -\exp(i\varphi) J_{m+1}(k_\perp \rho) \end{pmatrix}. \quad (39) \end{aligned}$$

Solution (37) is longitudinal: for it, $\omega^2 = c_1^2(k_\perp^2 + k_z^2)$; and solutions (38) and (39) are transverse: for them, $\omega^2 = c_t^2(k_\perp^2 + k_z^2)$.

6. Vibrations of an infinite rod with a free surface

To find the dispersion relation for a traveling wave propagating along an infinite circular cylinder of radius R with a free surface, we take a linear combination

$$a \mathbf{u}_{mq_\perp k_z}^{(1)} + b \mathbf{u}_{mQ_\perp k_z}^{(1)} + c \mathbf{u}_{mQ_\perp k_z}^{(2)} \quad (40)$$

of independent solutions of Eqn (22) that correspond to the given frequency ω , the projection of total angular momentum m , and the wave vector along the cylinder axis k_z , and require that the associated traction vector vanish on the lateral cylinder surface, i.e., at $\rho = R$. The solutions entering (40) are given by expressions (37)–(39). The longitudinal solution is taken with the wave number

$$k_\perp = \sqrt{\left(\frac{\omega}{c_1}\right)^2 - k_z^2} \equiv q_\perp,$$

and the transverse ones with the wave number

$$k_\perp = \sqrt{\left(\frac{\omega}{c_t}\right)^2 - k_z^2} \equiv Q_\perp.$$

The components of stress acting on an element of the lateral cylinder surface per unit area, expressed in cylindrical coordinates, are [25]

$$\begin{aligned} F_{m\rho} &= \frac{\rho_M \exp[i(k_z z + m\varphi)]}{\sqrt{2\pi}} \\ &\times \left\{ a \left[(c_1^2 - 2c_t^2) \sqrt{q_\perp^2 + k_z^2} J_m(q_\perp R) \right. \right. \\ &\left. \left. - \frac{2c_t^2}{\sqrt{q_\perp^2 + k_z^2}} \frac{d^2 J_m(q_\perp R)}{dR^2} \right] - b \frac{2c_t^2 k_z}{Q_\perp \sqrt{Q_\perp^2 + k_z^2}} \frac{d^2 J_m(Q_\perp R)}{dR^2} \right. \\ &\left. - c \frac{2mc_t^2}{Q_\perp} \frac{d}{dR} \left(\frac{J_m(Q_\perp R)}{R} \right) \right\}, \quad (41) \end{aligned}$$

$$\begin{aligned} F_{m\varphi} &= \frac{i\rho_M c_t^2 \exp[i(k_z z + m\varphi)]}{\sqrt{2\pi}} \\ &\times \left[a \frac{2m}{\sqrt{q_\perp^2 + k_z^2} R} \left(\frac{J_m(q_\perp R)}{R} - \frac{dJ_m(q_\perp R)}{dR} \right) \right. \\ &+ b \frac{2k_z m}{\sqrt{Q_\perp^2 + k_z^2} Q_\perp R} \left(\frac{J_m(Q_\perp R)}{R} - \frac{dJ_m(Q_\perp R)}{dR} \right) \\ &\left. - c Q_\perp \left(\frac{2}{Q_\perp^2} \frac{d^2 J_m(Q_\perp R)}{dR^2} + J_m(Q_\perp R) \right) \right], \quad (42) \end{aligned}$$

$$\begin{aligned} F_{mz} &= \frac{i\rho_M c_t^2 \exp[i(k_z z + m\varphi)]}{\sqrt{2\pi}} \left[-a \frac{2k_z}{\sqrt{q_\perp^2 + k_z^2}} \frac{dJ_m(q_\perp R)}{dR} \right. \\ &\left. + b \frac{Q_\perp^2 - k_z^2}{Q_\perp \sqrt{Q_\perp^2 + k_z^2}} \frac{dJ_m(Q_\perp R)}{dR} - cmk_z \frac{J_m(Q_\perp R)}{Q_\perp R} \right]. \quad (43) \end{aligned}$$

The dispersion relation for vibrational modes in the rod follows from the condition $F_{m\rho} = F_{m\varphi} = F_{mz} = 0$. Because of its cumbersome character, we do not write it explicitly in the general form, and limit ourselves to an analysis of the case $m = 0$. For $m = 0$, expressions (41) and (43) do not contain a contribution from solution (39), whereas expression (42) does not contain contributions from (37) and (38). For this reason, solutions (37)–(39) are mixed via boundary conditions only partly. Transverse modes coming from solution (39) correspond to torsional vibrations. For their dispersion, we obtain

$$J_2(Q_\perp R) = 0. \quad (44)$$

Notably, this gives the solution $Q_\perp = 0$ or $\omega = c_t k_z$, which corresponds to torsional vibrations with linear dispersion. The same result for a rod with a circular cross section follows from the thin rod theory [1].

Dispersion relations for the remaining vibrational modes corresponding to $m = 0$ can be found from the equation

$$\begin{aligned} &\left[\left(1 - 2 \frac{c_t^2}{c_1^2} \right) \omega^2 J_0(q_\perp R) + 2c_t^2 q_\perp \frac{dJ_1(q_\perp R)}{dR} \right] \\ &\times (Q_\perp^2 - k_z^2) J_1(Q_\perp R) + 4c_t^2 k_z^2 q_\perp J_1(q_\perp R) \frac{dJ_1(Q_\perp R)}{dR} = 0. \quad (45) \end{aligned}$$

Equation (45) was first published by Pochhammer [5] and took his name [9]. Vibrations of a cylindrical rod were also considered in the work by Chree [4] already cited in Section 4. The left-hand side of Eqn (45) can be regarded as a function of $Q_\perp R$. Then, for

$$0 < Q_\perp < k_z \sqrt{\frac{c_1^2}{c_t^2} - 1}, \quad (46)$$

q_\perp becomes purely imaginary. In this domain, Eqn (45) should be modified via the substitution $q_\perp \rightarrow i\kappa_\perp$, $J_m(q_\perp R) \rightarrow i^m I_m(\kappa_\perp R)$, where $I_m(x)$ is the modified Bessel function of order m .

We note that in calculating the dispersion relation for a flexural wave, which has a quadratic character for small k_z and corresponds to $|m| = 1$, both q_\perp and Q_\perp become imaginary.

Among vibrational modes whose frequencies satisfy Eqn (45), we can single out a longitudinal wave of expansion with a linear dispersion relation for small k_z . This dependence can be obtained by expanding the Bessel functions in Eqn (45) up to linear terms,

$$\omega = \sqrt{\frac{3c_1^2 - 4c_t^2}{c_1^2 - c_t^2}} c_t k_z = \sqrt{\frac{E}{\rho_M}} k_z \equiv \omega_0, \quad (47)$$

where E is Young's modulus. The same dependence occurs in the thin rod theory [1]. If we now substitute $\omega^2 = \omega_0^2 + \Delta(\omega^2)$ in (45) and expand in a series up to the terms linear in $\Delta(\omega^2)$ and quadratic in $Q_\perp R$ and $q_\perp R$, we obtain $2\Delta(\omega^2) = -\omega_0^2 \sigma^2 (k_z R)^2$ or

$$\omega = \omega_0 \left(1 - \frac{\sigma^2 (k_z R)^2}{4} \right), \quad (48)$$

where

$$\sigma = \frac{c_1^2 - 2c_t^2}{2(c_1^2 - c_t^2)} \quad (49)$$

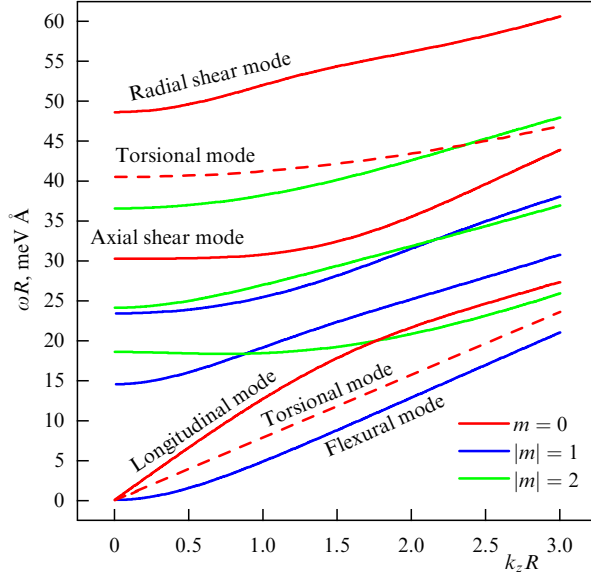


Figure 2. (Color online.) Dispersion curves for the first several mixed modes corresponding to $m = 0$ (solid red lines), $|m| = 1$ (blue lines), and $|m| = 2$ (green lines) of a gold cylindrical rod with radius R obtained in the framework of the isotropic model. The red dashed lines plot dispersion curves for torsional vibrations that correspond to $m = 0$.

is the Poisson ratio [1]. This result is known as Rayleigh's correction to the frequency of longitudinal waves in thin rods [9].

Figure 2 shows dispersion curves for various modes of vibrations in a gold rod having the form of an infinite circular cylinder with a radius R , predicted by the isotropic model. The values $c_1 = 3.24 \times 10^5$ cm s⁻¹ and $c_t = 1.2 \times 10^5$ cm s⁻¹ were taken for the speeds of sound. Shown are the first two solutions of Eqn (44), the first three solutions of Eqn (45) for mixed vibrations with $m = 0$, and the first three modes for $|m| = 1$ and $|m| = 2$.

A very elegant experiment by Zemanek [26] in which vibration modes were excited in a macroscopic aluminum cylinder 3 m in length and 3 cm in diameter is worth mentioning. Owing to its macroscopic size, the sample was polycrystalline and was very well described by the isotropic model. In this experiment, the dispersion curves predicted by the model were confirmed with high accuracy.

Nanoparticles of semiconductors and metals having a shape close to a circular cylinder, known as nanorods, can also be produced by the methods of colloidal chemistry. Review [24] describes experiments where the longitudinal expansion mode and radial 'breathing' mode were excited in nanorods of noble metals by femtosecond laser pulses. The finiteness of the lengths of such nanorods can be taken into account by quantization of the values of wave number $k_z = \pi n_z / L_z$, where L_z is the nanorod length and n_z is a natural number. What was said in Section 4 about the applicability of the isotropic model to describing vibrations in spherical particles is equally applicable to nanorods.

Vibrational modes in nanowires of GaN with a hexagonal cross section, produced by the method of molecular-beam epitaxy, were studied in [27] with the help of Mandelshtam–Brillouin scattering spectroscopy. Vibrational modes in such nanowires can also be approximately described with the help of the isotropic model.

7. Vibrations of an infinite plate with free surfaces

Dispersion relations for an outgoing cylindrical wave propagating in an infinite plate confined between two planes $z = \pm h/2$ are obtained by imposing no-stress conditions on the bounding surfaces for the linear combination

$$a_+ \mathbf{u}_{mk_\perp q_z}^{(1)} + a_- \mathbf{u}_{mk_\perp -q_z}^{(1)} + b_+ \mathbf{u}_{mk_\perp Q_z}^{(t1)} + b_- \mathbf{u}_{mk_\perp -Q_z}^{(t1)} + c_+ \mathbf{u}_{mk_\perp Q_z}^{(t2)} + c_- \mathbf{u}_{mk_\perp -Q_z}^{(t2)} \quad (50)$$

of solutions (37)–(39) of Eqn (22) corresponding to the given frequency ω , the total angular momentum projection m , and the wave number k_\perp in the plate plane. In this case, q_z and Q_z in expression (50) satisfy the conditions

$$q_z^2 = \frac{\omega^2}{c_t^2} - k_\perp^2, \quad (51)$$

$$Q_z^2 = \frac{\omega^2}{c_t^2} - k_\perp^2. \quad (52)$$

We need expressions for the force due to stresses acting on a surface element perpendicular to the z axis, per unit surface. In a cylindrical coordinate system, the components of this force corresponding to the terms with subscripts $+$ in coefficients in expression (50) take the form

$$F_{m+\rho} = \frac{i\rho_M c_t^2 \exp(im\varphi)}{\sqrt{2\pi}} \left[-a_+ \frac{2q_z}{\sqrt{k_\perp^2 + q_z^2}} \times \frac{dJ_m(k_\perp\rho)}{d\rho} \exp(iq_z z) + b_+ \frac{k_\perp^2 - Q_z^2}{k_\perp \sqrt{k_\perp^2 + Q_z^2}} \times \frac{dJ_m(k_\perp\rho)}{d\rho} \exp(iQ_z z) - c_+ m Q_z \frac{J_m(k_\perp\rho)}{k_\perp \rho} \exp(iQ_z z) \right], \quad (53)$$

$$F_{m+\varphi} = \frac{\rho_M c_t^2 \exp(im\varphi)}{\sqrt{2\pi}} \left[a_+ \frac{2mq_z}{\sqrt{k_\perp^2 + q_z^2}} \frac{J_m(k_\perp\rho)}{\rho} \exp(iq_z z) + b_+ \frac{m(Q_z^2 - k_\perp^2)}{k_\perp \sqrt{k_\perp^2 + Q_z^2}} \frac{J_m(k_\perp\rho)}{\rho} \exp(iQ_z z) + c_+ \frac{Q_z}{k_\perp} \frac{dJ_m(k_\perp\rho)}{d\rho} \exp(iQ_z z) \right], \quad (54)$$

$$F_{m+z} = \frac{\rho_M \exp(im\varphi) J_m(k_\perp\rho)}{\sqrt{2\pi}} \left[a_+ \left(c_t^2 \sqrt{k_\perp^2 + q_z^2} - \frac{2c_t^2 k_\perp^2}{\sqrt{k_\perp^2 + q_z^2}} \right) \exp(iq_z z) - b_+ \frac{2c_t^2 Q_z k_\perp}{\sqrt{k_\perp^2 + Q_z^2}} \exp(iQ_z z) \right]. \quad (55)$$

The components \mathbf{F}_{m-} follow after replacing $q_z \rightarrow -q_z$, $Q_z \rightarrow -Q_z$, and the subscript $+$ with the $-$.

We impose the boundary condition that $\mathbf{F}_{m+} + \mathbf{F}_{m-}$ vanish at $z = \pm h/2$. It can be readily seen that solutions $\mathbf{u}_{mk_\perp \pm Q_z}^{(t2)}$, describing shear waves, do not become mixed with the other solutions by these boundary conditions. The dispersion relation for shear waves takes the form

$$\sin(Q_z h) = 0. \quad (56)$$

Its solutions include one with $Q_z = 0$ describing a transverse acoustic wave with a linear dispersion $\omega = c_t k_\perp$. Similar solutions are obtained in the theory of thin plates [1]. The shear character of such a wave is reflected in vibrations being

transverse and taking place in the plate plane. Other solutions are obtained for $Q_z = \pi n/h$, where n is a natural number. For them,

$$\omega = c_t \sqrt{\frac{\pi^2 n^2}{h^2} + k_\perp^2}. \quad (57)$$

The boundary conditions connecting the solutions $\mathbf{u}_{mk_\perp \pm Q_z}^{(1)}$ and $\mathbf{u}_{mk_\perp \pm Q_z}^{(2)}$ lead to the dispersion equation

$$\begin{aligned} & \left[(\omega^2 - 2c_t^2 k_\perp^2)^4 + 16 \frac{c_t^6}{c_l^2} (\omega^2 - c_t^2 k_\perp^2) (\omega^2 - c_t^2 k_\perp^2) k_\perp^4 \right] \\ & \times \sin(q_z h) \sin(Q_z h) + 16c_t^4 k_\perp^2 q_z Q_z (\omega^2 - 2c_t^2 k_\perp^2)^2 \\ & \times \left[\sin^2 \frac{q_z h}{2} \cos^2 \frac{Q_z h}{2} + \sin^2 \frac{Q_z h}{2} \cos^2 \frac{q_z h}{2} \right] = 0. \end{aligned} \quad (58)$$

It is assumed that when q_z^2 in Eqn (51) becomes negative, the transformation $q_z \rightarrow i\kappa_z$, $\sin(q_z h) \rightarrow i \sinh(\kappa_z h)$ and so on is performed. The same concerns the case $Q_z^2 < 0$.

Waves with dispersion described by Eqn (58) have a mixed character. Their plane analogs have the name Lamb waves [28]. Ultrasonic Lamb waves are widely used in technology [28]. They are used in ultrasonic defectoscopy to determine elastic and thermoelastic characteristics of plate-like samples and to construct delay lines.

We divide both sides of (58) by

$$\cos^2 \frac{Q_z h}{2} \sin^2 \frac{q_z h}{2}$$

and use Eqns (51) and (52). We find

$$\begin{aligned} & \left[(k_\perp^2 - Q_z^2)^4 + 16q_z^2 Q_z^2 k_\perp^4 \right] x \\ & + 4k_\perp^2 q_z Q_z (k_\perp^2 - Q_z^2)^2 (1 + x^2) = 0, \end{aligned} \quad (59)$$

where

$$x = \frac{\tan(Q_z h/2)}{\tan(q_z h/2)}.$$

Solving quadratic equation (59) for x , we obtain two solutions:

$$\frac{\tan(Q_z h/2)}{\tan(q_z h/2)} = -\frac{4k_\perp^2 q_z Q_z}{(k_\perp^2 - Q_z^2)^2}, \quad (60)$$

$$\frac{\tan(Q_z h/2)}{\tan(q_z h/2)} = -\frac{(k_\perp^2 - Q_z^2)^2}{4k_\perp^2 q_z Q_z}. \quad (61)$$

Equations (60) and (61), which were obtained in Refs [6–8], are known as Rayleigh–Lamb equations [9] for the dispersion of respectively symmetric and antisymmetric plane waves (Lamb waves) in a plate.

We return to the analysis of Eqn (58). Substituting $\omega = v_l k_\perp$ in (58) and expanding trigonometric functions in series up to linear terms, we obtain

$$v_l^2 = 4c_t^2 \left(1 - \frac{c_t^2}{c_l^2} \right). \quad (62)$$

Here, v_l is the propagation speed of a longitudinal acoustic wave in the plate plane, known from the theory of thin plates [1]. If we now substitute $\omega = \gamma k_\perp^2$ in (58) and expand trigonometric functions up to cubic terms, we obtain

$$\gamma^2 = c_t^2 \left(1 - \frac{c_t^2}{c_l^2} \right) \frac{h^2}{3} \equiv \frac{h^2 v_l^2}{12}, \quad (63)$$

where γ is the dispersion coefficient of flexural waves known from the theory of thin plates [1].

Elastic waves whose propagation can be described in the framework of thin plate theory [1] are limited to transverse acoustic waves, longitudinal acoustic waves, and flexural waves with quadratic dispersion. Thus, there are three parameters in this theory, c_t , v_l , and γ . Accordingly, relying on symmetry considerations, we can write an analog of the operator \hat{A} from Eqn (22) for a thin plate [29]:

$$\begin{aligned} \hat{A}_{\text{plate}} = & \frac{v_l^2 - c_t^2}{2} \left(\nabla_x^2 \hat{S}_+^2 + \nabla_y^2 \hat{S}_-^2 \right) \\ & - \frac{v_l^2 + c_t^2}{2} \hat{S}_z^2 \nabla_\perp^2 - \gamma^2 \left(\hat{S}_z^2 - \hat{I} \right) \nabla_\perp^4, \end{aligned} \quad (64)$$

where $\nabla_\pm = \nabla_x \pm i\nabla_y$, $\nabla_\perp^2 = \nabla_x^2 + \nabla_y^2$, $\hat{S}_\pm = \mp(\hat{S}_x \pm i\hat{S}_y)/\sqrt{2}$. These equations of motion can be used to describe low-frequency vibrations in graphene, taking the parameters c_t , v_l , and γ from an experiment or microscopic computations. Next, we can trace how the operator \hat{A}_{plate} changes under rolling a graphene sheet into a nanotube and derive the corresponding equations of motion [29]. If expression (63) is used for γ , then Donnell's equations describing vibrational motion in thin cylindrical shells follow [30]. Dispersion relations for low-frequency vibrations of nanotubes can be readily derived from their equations of motion [29].

However, solutions of Eqn (58) are not limited to waves with linear and quadratic dispersion. For $k_\perp = 0$, Eqn (58) becomes

$$\sin \frac{\omega h}{c_l} \sin \frac{\omega h}{c_t} = 0, \quad (65)$$

giving $\omega = c_l \pi n/h$ and $\omega = c_t \pi n/h$. The first of these equations for $n = 1$ corresponds to the frequency of the ‘breathing’ mode in a plate. This mode is purely longitudinal. Its vibrations cause changes to the plate volume and its displacements are perpendicular to the plate plane. The fact that the left-hand side of (65) is the product of two factors implies that the vibrational modes are no longer mixed for $k_\perp = 0$ and that their displacement fields are either longitudinal or transverse.

Because the Bessel functions have the property $J_m(0) = 0$ for any integer m except $m = 0$, it can be concluded from Eqns (37)–(39) that for $k_\perp = 0$ the longitudinal modes correspond to $m = 0$ and the transverse mode to $|m| = 1$. In this limit, solutions (38) and (39) become equivalent. For $k_\perp > 0$, all vibrational modes are degenerate in m , similarly to plane waves in a plate, which are degenerate with respect to their propagation direction.

Recently, chemists have learned how to synthesize semiconductor monocrystal nanoplatelets with a thickness of several atomic layers controlled with atomic accuracy [31]. For example, a nanoplatelet of CdSe has a crystal structure of sphalerite (zinc blende), but in the first approximation its vibrational modes can be described in the framework of the isotropic model neglecting crystal anisotropy.

Figure 3 displays dispersion curves for the first several mixed (red curves) and shear (blue curves) vibrational modes in a CdSe nanoplatelet with a thickness of three monolayers ($h = 9 \text{ \AA}$). We used averaged parameters for speeds of sound $c_l = 3.7 \times 10^5 \text{ cm s}^{-1}$ and $c_t = 1.54 \times 10^5 \text{ cm s}^{-1}$ (which give $v_l = 2.67 \times 10^5 \text{ cm s}^{-1}$) and the value $a = 6 \text{ \AA}$ for the lattice constant. The values of frequencies are given in energy units and correspond to $\hbar\omega$. The dashed lines in Fig. 3 show the

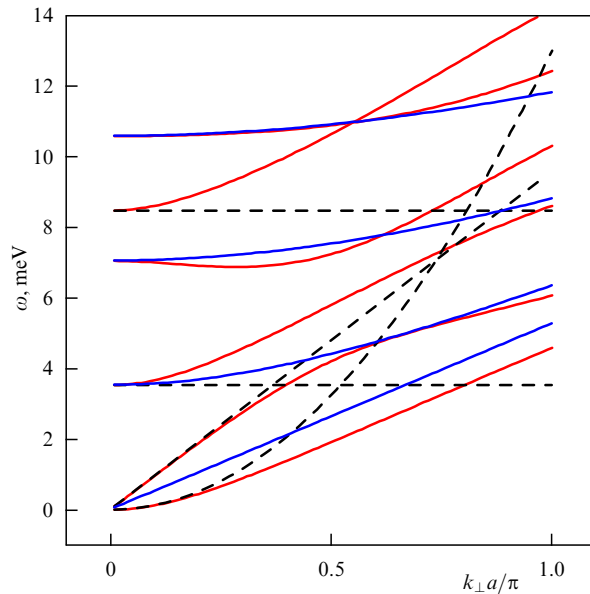


Figure 3. (Color online.) Dispersion curves for the first several mixed (red curves) and shear (blue curves) vibrational modes in a CdSe nanoplatelet with a thickness of three molecular layers computed in the framework of the isotropic model. The dashed lines show the dependences $\omega = hv_{\perp}k_{\perp}^2/\sqrt{12}$, $\omega = v_{\perp}k_{\perp}$, $\omega = c_{\perp}\pi/h$, and $\omega = c_{\perp}\pi/h$.

dependences $\omega = hv_{\perp}k_{\perp}^2/\sqrt{12}$, $\omega = v_{\perp}k_{\perp}$, $\omega = c_{\perp}\pi/h$, and $\omega = c_{\perp}\pi/h$.

8. Conclusions

Using the mathematical formalism of the quantum theory of angular momentum, the eigenfunctions of the total angular momentum operator can be constructed from the known eigenfunctions of the angular momentum operators entering the sum. We have demonstrated that this allows essential progress in constructing solutions of the second-order partial differential equation describing the propagation of elastic waves in a homogeneous isotropic medium in situations where the boundary conditions have spherical or axial symmetry. The subsequent solution of the elastic body vibration problem reduces to applying standard methods of elasticity theory. The quantum theory of angular momentum offers an understanding of the solution structure without resorting to direct computations and uncovers the physical meaning of parameters used to classify vibrational modes. Another advantage of such an approach is the fact that all vibrational modes follow from a unified treatment, eliminating the need to consider numerous particular cases.

Models of an isotropic elastic sphere, an infinite cylindrical rod, and an infinite plate are best suited to describing polycrystal bodies. Nevertheless, they prove to be extremely useful in describing vibrational modes in nanocrystals of various dimensions, even when the nanocrystals have a monocrystal structure.

This study was supported in part by the National Science Foundation (NSF-CREST grant HRD-1547754).

References

1. Landau L D, Lifshitz E M *Theory of Elasticity* (Oxford: Pergamon Press, 1986); Translated from Russian: *Teoriya Uprugosti* (Moscow: Nauka, 1987)
2. Jaerisch P J. *Reine Angew. Math.* **88** 131 (1880)
3. Lamb H *Proc. Lond. Math. Soc.* **s1-13** 189 (1882)
4. Chree C *Trans. Camb. Phil. Soc.* **14** 250 (1889)
5. Pochhammer L J. *Reine Angew. Math.* **81** 324 (1876)
6. Rayleigh (Lord) *Proc. Lond. Math. Soc.* **s1-20** 225 (1888)
7. Lamb H *Proc. Lond. Math. Soc.* **s1-21** 70 (1889)
8. Lamb H *Proc. R. Soc. Lond. A* **93** 114 (1917)
9. Graff K F *Wave Motion in Elastic Solids* (New York: Dover Publ., 1991)
10. Eringen A C, Suhubi E S *Elastodynamics Vol. 2 Linear Theory* (New York: Academic Press, 1975)
11. Lapwood E R, Usami T *Free Oscillations of the Earth* (Cambridge: Cambridge Univ. Press, 1981)
12. Varshalovich D A, Moskalev A N, Khersonskii V K *Quantum Theory of Angular Momentum* (Singapore: World Scientific, 1988); Translated from Russian: *Kvantovaya Teoriya Uglovogo Momenta* (Leningrad: Nauka, 1975)
13. Wallace P R *Mathematical Analysis of Physical Problems* (New York: Dover Publ., 1984)
14. Mattis D C *The Theory of Magnetism Made Simple* (Singapore: World Scientific, 2006)
15. Goupalov S V *Phys. Rev. B* **68** 125311 (2003)
16. Berestetskii V B, Lifshitz E M, Pitaevskii L P *Quantum Electrodynamics* (Oxford: Pergamon Press, 1982); Translated from Russian: *Kvantovaya Elektrodinamika* (Moscow: Nauka, 1989)
17. Goupalov S V, Saviot L, Duval E *Phys. Rev. B* **74** 197401 (2006)
18. Gupalov S V, Merkulov I A *Phys. Solid State* **41** 1349 (1999); *Fiz. Tverd. Tela* **41** 1473 (1999)
19. Poisson S D *Mémoire l'Acad. Sci. l'Inst. France* **8** 357 (1829)
20. Ekimov A I, Onushchenko A A *JETP Lett.* **34** 345 (1981); *Pis'ma Zh. Eksp. Teor. Fiz.* **34** 363 (1981)
21. Murray C B, Kagan C R, Bawendi M G *Annu. Rev. Mater. Sci.* **30** 545 (2000)
22. Duval E *Phys. Rev. B* **46** 5795(R) (1992)
23. Saviot L, Mermet A, Duval E "Acoustic vibrations in nanoparticles", in *Handbook of Nanophysics. Nanoparticles and Quantum Dots* (Ed. K D Sattler) (Boca Raton: CRC Press, 2011)
24. Hartland G V *Chem. Rev.* **111** 3858 (2011)
25. Goupalov S V *Nano Lett.* **14** 1590 (2014)
26. Zemanek J (Jr.) *J. Acoust. Soc. Am.* **51** 265 (1972)
27. Johnson W L et al. *Nanotechnology* **23** 495709 (2012)
28. Viktorov I A *Rayleigh and Lamb Waves: Physical Theory and Applications* (New York: Plenum Press, 1967); Translated from Russian: *Fizicheskie Osnovy Primeneniya Ul'trazvukovykh Voln Releya i Lemba v Tekhnike* (Moscow: Nauka, 1966)
29. Goupalov S V *Phys. Rev. B* **71** 085420 (2005)
30. Kraus H *Thin Elastic Shells* (New York: Wiley, 1967)
31. Nasilowski M et al. *Chem. Rev.* **116** 10934 (2016)